JOURNAL OF VIROLOGY, June 2005, p. 6690–6702 Vol. 79, No. 11
0022-538X/05/$08.00+0 doi:10.1128/JVI.79.11.6690–6702.2005

Receptor Binding, Fusion Inhibition, and Induction of Cross-Reactive Neutralizing Antibodies by a Soluble G Glycoprotein of *Hendra Virus*

Katharine N. Bossart,[1]† Gary Crameri,[2]‡ Antony S. Dimitrov,[1]‡ Bruce A. Mungall,[2]‡ Yan-Ru Feng,[1] Jared R. Patch,[1] Anil Choudhary,[1] Lin-Fa Wang,[2] Bryan T. Eaton,[2] and Christopher C. Broder[1]*

Department of Microbiology and Immunology, Uniformed Services University, Bethesda, Maryland 20814,[1] and CSIRO Livestock Industries, Australian Animal Health Laboratory, Geelong, Victoria 3220, Australia[2]

Received 17 September 2004/Accepted 2 February 2005

***Hendra virus* (HeV) and *Nipah virus* (NiV) are closely related emerging viruses comprising the *Henipavirus* genus of the *Paramyxovirinae*, which are distinguished by their ability to cause fatal disease in both animal and human hosts. These viruses infect cells by a pH-independent membrane fusion event mediated by their attachment (G) and fusion (F) glycoproteins. Previously, we reported on HeV- and NiV-mediated fusion activities and detailed their host-cell tropism characteristics. These studies also suggested that a common cell surface receptor, which could be destroyed by protease, was utilized by both viruses. To further characterize the G glycoprotein and its unknown receptor, soluble forms of HeV G (sG) were constructed by replacing its cytoplasmic tail and transmembrane domains with an immunoglobulin κ leader sequence coupled to either an S-peptide tag ($sG_{S\text{-}tag}$) or myc-epitope tag ($sG_{myc\text{-}tag}$) to facilitate purification and detection. Expression of sG was verified in cell lysates and culture supernatants by specific affinity precipitation. Analysis of sG by size exclusion chromatography and sucrose gradient centrifugation demonstrated tetrameric, dimeric, and monomeric species, with the majority of the sG released as a disulfide-linked dimer. Immunofluorescence staining revealed that sG specifically bound to HeV and NiV infection-permissive cells but not to a nonpermissive HeLa cell line clone, suggesting that it binds to virus receptor on host cells. Preincubation of host cells with sG resulted in dose-dependent inhibition of both HeV and NiV cell fusion as well as infection by live virus. Taken together, these data indicate that sG retains important native structural features, and we further demonstrate that administration of sG to rabbits can elicit a potent cross-reactive neutralizing antibody response against infectious HeV and NiV. This HeV sG glycoprotein will be exceedingly useful for structural studies, receptor identification strategies, and vaccine development goals for these important emerging viral agents.**

Two newly recognized and closely related paramyxoviruses have been identified from cases of severe respiratory and encephalitic diseases in animals and humans; these viruses are known now as *Hendra virus* (HeV) and *Nipah virus* (NiV) (reviewed in reference 15). HeV appeared in eastern Australia in 1994 and was transmitted to humans by close contact with infected horses; NiV emerged in 1998 to 1999 in Malaysia and was primarily passed from infected pigs to humans as well as several other animal species (reviewed in references 12 and 39). Both are currently classified as biological safety level 4 (BSL-4) pathogens and are remarkable among the paramyxoviruses in their ability to infect and cause potentially fatal disease in a number of host species, including humans. HeV and NiV are genetically closely related yet distinct from all other paramyxovirus family members and have been reclassified into the new *Henipavirus* genus (40). In addition to the initial NiV outbreak, there have been four other suspected incidents: one in the Sarawak area, Borneo, Malaysia, in 2000; two in west Bengal, India; and a fourth in Bangladesh in 2001. Most recently, both NiV and HeV continue to make their presence known: in early 2004 two NiV outbreaks in Bangladesh have been confirmed, totaling some 53 human cases of infection, and HeV reappeared in northern Australia in late 2004, with two cases of fatal infection in horses and one nonfatal human case (2). Several significant observations in the most recent NiV outbreaks have been made, including a higher incidence of acute respiratory distress syndrome, possibly a higher incidence of person-to-person transmission, significantly higher case fatality rates (60 to 75%), and no direct link to infected livestock or domestic animals (1, 3, 9, 17). The development of therapeutic or intervention strategies to deal with these emerging viral agents is now of importance.

Paramyxoviruses are negative-sense RNA-containing enveloped viruses and contain two major membrane-anchored envelope glycoproteins that are required for infection of a receptive host cell. All members contain an F glycoprotein, which mediates pH-independent membrane fusion between the virus and its host cell, while the second attachment glycoprotein can be either a hemagglutinin-neuraminidase protein (HN), a hemagglutinin protein (H), or a G protein, depending on the particular virus (reviewed in reference 24). The F proteins are type I membrane glycoproteins existing as trimeric oligomers with considerable hydrophobicity, while the attachment glycoproteins are oligomeric type II membrane glycoproteins, and evidence has shown that both dimeric and/or tetrameric (a dimer of dimers) configurations exist from studies on the HN glycoprotein of Newcastle disease virus and simian virus 5

* Corresponding author. Mailing address: Department of Microbiology and Immunology, F. Edward Hébert School of Medicine, Uniformed Services University of the Health Sciences, 4301 Jones Bridge Road, Bethesda, MD 20814-4799. Phone: (301) 295-3401. Fax: (301) 295-1545. E-mail: cbroder@usuhs.mil.

† Present address: CSIRO Livestock Industries, Australian Animal Health Laboratory, Geelong, Victoria 3220, Australia.

‡ G.C., A.S.D., and B.A.M. contributed equally.

(SV5) and the H glycoprotein of measles virus (14, 26, 33, 36, 37).

HeV and NiV have a G attachment glycoprotein which lacks both hemagglutinin and neuraminidase activities. Previously, we devised a quantitative assay for studying the structural and functional characteristics of HeV and NiV glycoprotein-mediated membrane fusion (reviewed in references 5 and 16) and demonstrated a requirement for both glycoproteins for efficient fusion. We also identified potent heptad peptide-based fusion inhibitors against HeV and NiV (6, 7). Both HeV- and NiV-mediated fusion exhibited broad species tropism which parallels both natural and experimental virus infections of animals. HeV and NiV also possessed the same fusion tropism activities in greater than 25 different cell lines examined to date and also possess proportional cell fusion activities for each receptor-positive cell line tested (6, 7). Several cell lines nonpermissive for fusion, some derived from the same animal species, have been identified, and protease treatment of permissive cells has been shown to abolish HeV-mediated fusion, suggesting a cell surface protein is used as the virus receptor (6, 7).

To further characterize the viruses' G glycoprotein and its unknown host cell receptor, we have developed epitope-tagged versions of soluble HeV G ($sG_{S\text{-}tag}$ and $sG_{myc\text{-}tag}$) which are expressed and secreted from cells using recombinant vaccinia virus vectors. Here we detail several important biological characteristics of the HeV sG glycoprotein. Our data indicate that sG is released from cells in monomeric, dimeric, and tetrameric forms and that the dimer is the predominant species produced and is disulfide linked. Purified sG was capable of binding to fusion-permissive cells and not to nonpermissive cells, and it could efficiently inhibit both HeV- and NiV-mediated fusion in a dose-dependent manner as well as block live HeV and NiV infection. We also show that administration of sG emulsified with adjuvant in rabbits is capable of eliciting a polyclonal antibody response that potently neutralizes HeV and NiV infection in culture. This is the first report of an engineered full-length ectodomain of a paramyxovirus type II membrane G glycoprotein and, taken together, our findings indicate that sG retains several important native structural features, suggesting it may be a useful vaccine component for these important emerging viral agents.

MATERIALS AND METHODS

Cells and culture conditions. A HeLa cell line derivative was provided by Anthony Maurelli, Uniformed Services University. Vero cells were provided by Alison O'Brien, Uniformed Services University. The human glioblastoma cell line U373-MG was provided by Adam P. Geballe, Fred Hutchinson Cancer Research Center (23). The human head and neck carcinoma PCI 13 cell line was the gift of Ernest Smith, Vaccinex, Inc. HeLa and U373 cells were maintained in Dulbecco's modified Eagle's medium (Quality Biologicals, Gaithersburg, MD) supplemented with 10% cosmic calf serum (HyClone, Logan, UT) and 2 mM L-glutamine (DMEM-10). PCI 13 cells were maintained in DMEM-10 supplemented with 10 mM HEPES (Quality Biologicals). Vero cells were maintained in Eagle's minimal essential medium (EMEM; Quality Biologicals) supplemented with 10% cosmic calf serum (HyClone) and 2 mM L-glutamine (EMEM-10). All cell cultures were maintained at 37°C in a humidified 5% CO_2 atmosphere.

Construction of soluble G glycoproteins. A HeV G (sHeV G) with the transmembrane-cytoplasmic tail deleted was constructed by PCR amplification of HeV G using primers sHGS, 5′-GTCGACCACCATGCAAAATTACACCAG AACGACTGATAAT-3′, and sHGAS, 5′-GTTTAAACGTCGACCAATCAAC TCTCTGAACATTGGGCAGGTATC-3′.

All PCRs were performed using Accupol DNA polymerase (PGS Scientifics Corp., Gaithersburg, MD). These primers generated a PCR product for the sHeV G open reading frame flanked by SalI sites. PCR products were gel purified (QIAGEN, Valencia, CA) and subcloned into the TOPO vector (Invitrogen Corp., Carlsbad, CA). The TOPO sHeV G construct was then subcloned into pSecTag2B (Invitrogen Corp.). The pSecTag-sHeVG construct was then modified by inserting either the S-peptide tag or a myc-epitope tag using complementary overlapping oligonucleotides as follows. Overlapping oligonucleotides were synthesized that encoded the sequence for the S-peptide along with KpnI and EcoRI restriction sites: SPEPS, 5′- CAAGGAGACCGCTGCTGCT AAGTTCGAACGCCAGCACATGGATTCT-3′; SPEPAS, 5′-AATTAGAAT CCATGTGCTGGCGTTCGAACTTAGCAGCAGCGGTCTCCTTGGTAC-3′. Overlapping oligonucleotides were synthesized that encoded the sequence for the myc epitope tag along with KpnI and EcoRI restriction sites: MTS, 5′-CG AACAAAAGCTCATCTCAGAAGAGGATCTG-3′; MTAS, 5′-AATTCAGA TCCTCTTCTGAGATGAGCTTTTGTTCGGTAC-3′. The annealed oligonucleotides were cloned into KpnI-EcoRI-digested pSeqTag2B-sHeV G to generate $sG_{S\text{-}tag}$ or $sG_{myc\text{-}tag}$. The HeV $sG_{S\text{-}tag}$ and $sG_{myc\text{-}tag}$ constructs were then subcloned into the vaccinia vector pMCO2 (10) to generate recombinant vaccinia viruses vKB16 ($sG_{S\text{-}tag}$) and vKB15 ($sG_{myc\text{-}tag}$).

Recombinant vaccinia viruses. For expression of recombinant $sG_{S\text{-}tag}$ or $sG_{myc\text{-}tag}$ glycoprotein, the following recombinant vaccinia viruses were generated and employed: vKB16 and vKB15. For expression of recombinant HeV and NiV F and G glycoproteins, the following recombinant vaccinia viruses were employed: vKB7 (NiV F), vKB6 (NiV G), vKB1 (HeV F), and vKB2 (HeV G) (6, 7). Bacteriophage T7 RNA polymerase was produced by infection with vTF7-3 (19). The *Escherichia coli lacZ* gene linked to the T7 promoter was introduced into cells by infection with vCB21R-LacZ (18).

Purification and analysis of soluble HeV G glycoproteins. HeLa cells were infected with vKB16 (multiplicity of infection [MOI] of 3) for 2 h. After infection the virus was removed and serum-free OptiMEM medium (Invitrogen Corp.) was added. After 36 h, the supernatants were removed and clarified by centrifugation. An S-protein column was poured with 15 ml of S-protein agarose (Novagen, Inc., San Diego, CA) in an XK26 column (Amersham Pharmacia Biotech, Piscataway, NJ), and the column was washed with 10 bed volumes of phosphate-buffered saline (PBS). The supernatant from vKB16-infected cells was passed over S-protein agarose, and the column was washed with 10 bed volumes of PBS. The $sG_{S\text{-}tag}$ was eluted with 1 bed volume of 0.2 M citrate, pH 2, into 20 ml of 1 M Tris, pH 8. The eluate was then concentrated using 30-kDA Centricon centrifugal filter units (Millipore, Billerica, MA). Protein concentrations were determined by sodium dodecyl sulfate-polyacrylamide gel electrophoresis (SDS-PAGE), Coomassie brilliant blue R-250 staining, and densitometry analysis with NIH Image 1.62 software by comparison to a standard amount of purified $sG_{S\text{-}tag}$ previously analyzed by quantitative amino acid analysis.

Molecular weight determinations. A Superdex 200 gel filtration column 10/300 (Amersham Pharmacia Biotech, Piscataway, NJ) was purchased. Void volume (Vo) was determined using blue dextran (1 mg/ml) in degassed PBS, pH 7.4 (Quality Biologicals, Inc., Gaithersburg, MD). A panel of high-molecular-weight protein markers (Amersham Pharmacia Biotech) was separated on a Superdex 200 column in PBS using an Amersham Pharmacia Biotech P-500 pump at a constant flow rate of 60 ml/h to determine their elution volumes (Ve). Each eluted fraction of 0.5 ml was collected at 30-s intervals and monitored by UV absorption at 280 nm. A Kav for each protein was calculated using the formula $Kav = (Ve - Vo)/(Vt - Vo)$, were Vt is the total column bed volume and Vo is the void volume, to generate a calibration curve. The $sG_{S\text{-}tag}$ was then separated on the calibrated column under conditions identical to those used for the protein markers, and their elution volumes (Ve) were determined. Kav values for fractions containing $sG_{S\text{-}tag}$ were calculated, and the molecular weights were determined. Fractions containing $sG_{S\text{-}tag}$ as determined by UV absorption were confirmed by SDS-PAGE and Coomassie G-250 staining.

Cell fusion assays. Fusion between envelope glycoprotein-expressing and target cells was measured by a reporter gene assay in which the cytoplasm of one cell population contained vaccinia virus-encoded T7 RNA polymerase and the cytoplasm of the other contained the *E. coli lacZ* gene linked to the T7 promoter; β-galactosidase (β-Gal) is synthesized only in fused cells (8, 29). Vaccinia virus-encoded proteins were produced by infecting cells at an MOI of 10 and incubating infected cells at 31°C overnight (4). Cell fusion reactions were conducted with the various cell mixtures in 96-well plates at 37°C. Typically, the ratio of envelope glycoprotein-expressing cells to target cells was 1:1 (2×10^5 total cells per well; 0.2-ml total volume). Cytosine arabinoside (40 μg/ml) was added to the fusion reaction mixture to reduce nonspecific β-Gal production (4). For quantitative analyses, Nonidet P-40 was added (0.5% final) at 2.5 h, and aliquots of the lysates were assayed for β-Gal at ambient temperature with the substrate chlorophenol red-D-galactopyranoside (Roche Diagnostics Corp.). For inhibition

by sG preparations, serial dilutions of sG were performed and added to target cell populations 30 min prior to the addition of effector cell populations. All assays were performed in duplicate, and fusion results were calculated and expressed as rates of β-Gal activity (change in optical density at 570 nm per minute × 1,000) (29).

Metabolic labeling and immunoprecipitation. For ^{35}S metabolic labeling of HeV glycoproteins expressed by recombinant vaccinia viruses, HeLa cells were infected at an MOI of 10. At 6 h postinfection, monolayers were washed, overlaid with methionine- and cysteine-free minimal essential medium (Invitrogen, Corp.) containing 2.5% dialyzed fetal calf serum (Invitrogen, Corp.) and 100 μCi of [^{35}S]methionine-cysteine (ProMix)/ml (Amersham Pharmacia Biotech, Piscataway, NJ), and incubated overnight. Supernatants were removed and clarified by centrifugation. Lysis of cells was performed in 100 mM Tris-HCl (pH 8.0), 100 mM NaCl, 1% Triton X-100, and the nuclei were removed by centrifugation. Typically, 2 μl of HeV antiserum (5), 1 μg of anti-c-*myc* monoclonal antibody (MAb) (9E10; Roche Molecular Biochemicals, Indianapolis, IN), or 50 μl of S-protein–agarose (50% slurry; Novagen) was utilized per immunoprecipitation mixture. The antigen and antibody mixtures were incubated for 1 h at 4°C, followed by addition of protein G-Sepharose 4B for 45 min. Complexes were washed twice with lysis buffer (100 mM Tris-HCl [pH 7.5], 100 mM NaCl, 1% Triton X-100) and once with DOC buffer (100 mM Tris-HCl [pH 8.0], 100 mM NaCl, 0.1% sodium deoxycholate, 0.1% SDS). Proteins were separated by SDS-PAGE (10%) and visualized by autoradiography.

Sucrose gradient analysis. The oligomeric forms of soluble and full-length HeV G glycoproteins were analyzed by sucrose gradient centrifugation. Nonmetabolically labeled material was used for the analysis of HeV $sG_{S\text{-}tag}$. The serum-free culture medium (12 ml of OptiMEM) containing $sG_{S\text{-}tag}$, produced from two T-162 cm^2 vKB16-infected HeLa cell culture flasks (40 h at 37°C), was collected, clarified by centrifugation, buffer-exchanged into PBS, and concentrated 40-fold using 30-kDA Centricon centrifugal filter units (Millipore, Billerica, MA). The final volume of 1 ml, containing approximately 100 μg, was divided in two equal portions of 0.5 ml each. One portion of the $sG_{S\text{-}tag}$ was cross-linked with the reducible reagent 3,3′-dithiobis-(sulfosuccinimidylpropionate) (DTSSP; Pierce Biotechnology, Rockford, IL) at a final concentration of 4 mM for 30 min at room temperature. The reaction was then quenched with 100 mM Tris (pH 7.5) for 15 min at room temperature, and the samples were layered onto the sucrose gradients.

For the analysis of full-length HeV G glycoprotein the protein was produced by infection of HeLa cell cultures using vKB2 and metabolically labeling with [^{35}S]methionine (Amersham Biosciences) for 18 h at 37°C. The culture was chased with complete medium for 2 h, and the cells were washed twice in PBS, recovered by using cell dissociation buffer (Invitrogen Corp.), and resuspended in 0.4 ml PBS. One half (0.2 ml) of the cell suspension was cross-linked with 1 mM DTSSP and incubated for 30 min at room temperature. The reaction was then quenched with 100 mM Tris, pH 7.5, for 15 min at room temperature. The cell surface cross-linked and un-cross-linked HeV G-expressing cells were lysed in Triton-X-containing buffer (100 mM Tris-HCl [pH 7.5], 100 mM NaCl, 1% Triton X-100, and protease inhibitor [Roche, Penzberg, Germany]) and clarified by centrifugation for 20 min at 13,000 rpm. The clarified cell lysates were then layered onto sucrose gradients.

Sucrose gradients were prepared as follows: 6 ml of 5% sucrose (100 mM Tris, 100 mM NaCl) was underlaid with 6 ml of 20% sucrose (100 mM Tris, 100 mM NaCl) in polyallomer 14- by 95-mm tubes (Beckman Coulter, Inc., Fullerton, CA). A linear sucrose gradient (5 to 20%) was then generated using a gradient master (Biocomp, Fredericton, NB, Canada) at an angle of 81.5° for 1 min 55 seconds and speed of 15 rpm. The cross-linked and un-cross-linked preparations of $sG_{S\text{-}tag}$ or full-length G were overlaid on top of the gradients and centrifuged at 40,000 rpm for 20 h using an SW40 rotor (Beckman, Inc.), and fractions (~0.5 ml) were collected from the bottom of the gradient using a Beckman fraction recovery system and automated fraction collector. The $sG_{S\text{-}tag}$ was precipitated from the fractions with S-protein–agarose (40 μl of a 50% slurry; Novagen) for 1 h at 4°C. Full-length G was precipitated from the fractions by using an anti-$sG_{S\text{-}tag}$ polyclonal mouse serum (0.5 μl per fraction) for 30 min at 4°C, followed by protein G-Sepharose beads. All precipitates were washed three times with precipitation buffer (100 mM Tris-HCl [pH 7.5], 100 mM NaCl, 1% Triton X-100). During the final wash the suspensions of beads from each fraction were divided into two tubes and centrifuged at 5,000 rpm for 1 min. The precipitates were then boiled in SDS sample buffer in the presence or absence of 5% β-mercaptoethanol. The precipitated material from each fraction was then analyzed by SDS-PAGE. Full-length G glycoprotein was analyzed using 3-to-8% Tris-acetate gradient gels (Invitrogen Corp.), and the $sG_{S\text{-}tag}$ glycoprotein was analyzed using 4-to-12% Tris-glycine gradient gels (Invitrogen Corp.). The metabolically labeled full-length G protein was visualized by autoradiography, and the nonlabeled $sG_{S\text{-}tag}$ was visualized by staining using SymplyBlue SaveStain. Coomassie G-250 (Invitrogen Corp.) images were obtained by digital scanning.

Indirect Immunofluorescence Assay (IFA). A total of 2×10^4 cells were plated per well into eight-well Lab-Tek II chamber slides (Nalge Nunc International, Naperville, IL) in the appropriate medium and incubated for 3 days at 37°C in a humidified 5% CO_2 atmosphere. The cells were fixed with acetone for 2 min and washed twice with PBS–0.05% Tween 20 (Sigma-Aldrich, St. Louis, MO). All wells were blocked with 200 μl PBS containing 3% bovine serum albumin (BSA; Sigma-Aldrich) and 10% normal goat serum (Sigma-Aldrich) (IFA buffer) for 2 h at 37°C. The cells were washed three times with PBS-Tween. Ten micrograms of $sG_{S\text{-}tag}$ in 200 μl of IFA buffer was added to each well and incubated at 37°C for 1 h. The cells were washed three times with PBS-Tween. HeV G peptide-specific antiserum (1:10,000) in 200 μl of IFA buffer was added to selected wells and incubated at 37°C for 1 h. The cells were washed three times with PBS-Tween. Alexa Fluor 488-conjugated donkey anti-rabbit immunoglobulin G (IgG)-specific antibodies (1:200; Molecular Probes, Eugene, OR) in 200 μl IFA buffer were added to each well and incubated at 37°C for 1 h. The cells were washed three times with PBS-Tween and allowed to air dry in the dark. The chambers were removed from the slides, and 90% glycerol–10% PBS-Tween was used as a mounting medium for the slide coverslips. Samples were examined with an Olympus BX60 system microscope with a BX-FLA reflected light fluorescence attachment and an Olympus U-M41001 filter. All images were obtained at an original magnification of ×40 with a SPOT RT charge-coupled device digital camera (Diagnostic Instruments, Inc., Sterling Heights, MI), and images were imported into Adobe Photoshop 7.0. Image size was adjusted individually, but brightness and contrast were only adjusted after all images had been merged.

HeV and NiV infection and IFA. All live virus experiments were conducted under strict biocontainment procedures in a BSL-4 laboratory. Vero cells were seeded into 96-well plates at 6×10^4 cells in 300 μl and grown to 90% confluence in EMEM-10 at 37°C under a humidified 5% CO_2 atmosphere. For inhibition experiments, the $sG_{S\text{-}tag}$ was diluted twofold in EMEM-10 and monolayers were preincubated with various $sG_{S\text{-}tag}$ concentrations for 30 min prior to virus inoculation. The medium was discarded, and 100 μl of diluted virus combined with the same amount of $sG_{S\text{-}tag}$ used in the preincubation was added per well and incubated at 37°C for 30 min. HeV and NiV were grown and titrated in Vero cells. The titer of HeV was 1.0×10^8 $TCID_{50}$/ml, and for NiV it was 3.0×10^7 $TCID_{50}$/ml. Virus dilutions were chosen to generate 50 plaques following adsorption of 100 μl of virus for 30 min at 37°C to Vero cell monolayers (1.5×10^3 50% tissue culture infective dose [$TCID_{50}$]/ml for HeV and 7.5×10^2 $TCID_{50}$/ml for NiV). Virus inoculum was removed, and 200 μl of $sG_{S\text{-}tag}$, at the same concentration as for both the preincubation and virus incubation, was added to each well and incubated at 37°C for 18 h. The culture medium was discarded the next day, and plates were immersed in ice-cold absolute methanol for 20 min prior to air drying outside the BSL-4 facility. Fixed chamber slides were either stored overnight at 4°C or immunolabeled immediately with antiphosphoprotein (P) monospecific antiserum. Wells were washed in 0.01 M PBS, pH 7.2, containing 1% BSA for 5 min. Forty microliters of anti-P antiserum (1:200 in PBS-BSA) was applied to each well and incubated at 37°C for 30 min. Slides were rinsed with PBS containing 0.05% Tween 20 and washed for 5 min in PBS-BSA. Forty microliters of fluorescein isothiocyanate (FITC)-labeled goat anti-rabbit antiserum (ICN Pharmaceuticals, Costa Mesa, CA) diluted 1:200 in PBS-BSA containing 4′,6′-diamidino-2-phenylindole (10 μg/ml) was then applied to each well and incubated at 37°C for 30 min. Wells were rinsed again with PBS containing 0.05% Tween 20 and washed for 5 min in PBS-BSA. Wells were overlaid with 100 μl glycerol-PBS (9:1) containing DABCO (25 μg/ml) and stored in the dark prior to imaging.

FITC immunofluorescence was visualized using an Olympus IX71 inverted microscope (Olympus Australia, Mt. Waverley, Australia) coupled to an Olympus DP70 high-resolution color camera, and all images were obtained at an original magnification of ×85. Image analysis was then performed using Analysis image analysis software (Soft Imaging System GmbH, Munster, Germany). Briefly, individual virus syncytia were detected by threshold analysis followed by "hole filling" and subsequently measured to determine the area of each syncytium. To ensure repeatability between images, all procedures were performed as a macro function with fixed parameters. Nine images were analyzed for each $sG_{S\text{-}tag}$ concentration, resulting in the collation of syncytial area data for between 9 and 79 foci per $sG_{S\text{-}tag}$ concentration (average, ~15). Measurements were collated, and nonlinear regression analysis was performed using GraphPad Prism software (GraphPad Software, San Diego, CA) to determine the 50% inhibitory concentration (IC_{50}).

HeV and NiV neutralization assay. All live virus experiments were conducted under strict biocontainment procedures in a BSL-4 laboratory. Antiserum was raised to $sG_{S\text{-}tag}$ in two rabbits by three inoculations each. For each rabbit, the

FIG. 1. HeV sG constructs. The HeV coding sequence with the transmembrane-cytoplasmic tail deleted was generated by PCR and cloned in frame into the pSecTag2B vector, which contained the Ig κ leader sequence. The modified epitope-tagged pSecTag2B vectors were subsequently generated using overlapping oligonucleotides and cloned in frame into pSecTag2B-HeV sG. The figure shows the S-peptide-tagged and c-*myc*-tagged versions of HeV sG. The linker amino acids were derived from vector sequences.

first inoculation contained 50 μg of $sG_{S\text{-}tag}$ in CSIRO triple adjuvant (60% [vol/vol] Montanide, 40% [vol/vol] $sG_{S\text{-}tag}$ [combined with Quil A, 3 mg/ml, and DEAE-dextran, 30 mg/ml] in water), in a total volume of 200 μl injected in two intramuscular sites. The second and third inoculations contained 25 μg of $sG_{S\text{-}tag}$ in CSIRO triple adjuvant in a total volume of 200 μl injected in two intramuscular sites. All injections were done 3 weeks apart. Sera were collected 2 weeks after the third inoculation. For both rabbits, prebleeds were also collected prior to inoculation. Sera were diluted in EMEM-10 by doubling dilution starting at 1:10. Fifty microliters of sera was added to wells in duplicate in a 96-well plate followed by 50 μl virus containing 200 $TCID_{50}$ of either HeV or NiV and incubated at 37°C for 30 min. A total of 2×10^4 Vero cells were added to all wells in 150 μl of EMEM-10 and incubated at 37°C for 4 days in a humidified 5% CO_2 atmosphere. Serum neutralization titers were determined by the presence of cytopathic effect (CPE) and recorded as the serum dilution where at least one of the duplicate wells showed no viral CPE.

RESULTS

Generation and expression of soluble and secreted G glycoproteins. The attachment glycoproteins of paramyxoviruses are type II membrane glycoproteins with a transmembrane domain proximal to the N terminus of the protein. It is thought that the protein's signal sequence for endoplasmic reticulum targeting located at the N terminus of the protein also overlaps with the molecule's transmembrane anchor domain (TM), making the construction of soluble and secreted forms more problematic. To circumvent these obstacles, we employed the pSecTag2 expression vector, which encodes the Ig κ leader sequence in combination with a HeV G cassette with the TM deleted, and we expressed them using recombinant vaccinia virus vectors. For ease of detection or purification of soluble protein, the pSecTag2-sHeV G vector was modified to contain either an S-peptide or c-*myc* epitope tag fused in frame in between the Ig κ leader sequence and sHeV G coding sequence. The design of the constructs also included two 15-amino acid linker elements, one between the Ig κ leader sequence and the epitope tag and the other between the epitope tag and sHeV G coding sequence. The Ig κ leader–S-peptide tag with TM deleted HeV G ($sG_{S\text{-}tag}$) and the Ig κ leader–myc tag with TM deleted HeV G ($sG_{myc\text{-}tag}$) fusions were 599 and 594 amino acids in length, respectively. Diagrams of the HeV $sG_{S\text{-}tag}$ and $sG_{myc\text{-}tag}$ constructs are shown in Fig. 1. The two sG constructs are identical with the exception of the epitope tags: the c-*myc* epitope tag is 10 amino acids, whereas the S-peptide sequence is 15 amino acids.

Shown in Fig. 2 are affinity precipitations of cell lysates and culture supernatants from metabolically labeled HeLa cells infected with WR (a control vaccinia virus), $sG_{S\text{-}tag}$, $sG_{myc\text{-}tag}$, or full-length HeV G-encoding vaccinia viruses. The various preparations were affinity precipitated with either virus-specific antiserum, anti-myc MAb, or S protein agarose as indicated in the figure. The anti-HeV antiserum and either the anti-myc MAb or the S-protein agarose were able to precipitate $sG_{myc\text{-}tag}$ and $sG_{S\text{-}tag}$, respectively, from both the lysates and the supernatants from the appropriate expressing cells. The cell lysate precipitates of $sG_{S\text{-}tag}$ and $sG_{myc\text{-}tag}$ had apparent molecular masses of ~80 kDa, similar to that seen with full-length G (7). The $sG_{S\text{-}tag}$ and $sG_{myc\text{-}tag}$ differ from full-length HeV G by 5 and 10 amino acid residues, respectively; thus, there was not a significant shift in the electrophoretic mobility of these sG glycoproteins. The $sG_{S\text{-}tag}$ and $sG_{myc\text{-}tag}$ glycoproteins precipitated from the cell culture supernatants had apparent molecular weights slightly larger than those of the sG glycoproteins recovered in the cell lysates or full-length HeV G. We speculate that this could be due to a putative N-linked glycosylation site located at the beginning of the protein's predicted ectodomain that may not be available for posttranslation modification in full-length membrane-anchored G because of its proximity to the TM domain. Previous studies have demonstrated that removal of this potential N-linked glycosylation site by mutagenesis had no effect on expression or function of full-length HeV G or on its apparent molecular weight (K. N. Bossart and C. C. Broder, unpublished observations). These observations suggest that this site is not normally modified, but in the context of the soluble form of the protein with TM deleted, it may be accessible, and such alteration is apparent when comparing sG that has been released from cells to the G glycoprotein still present within the cell. However, since both epitope-tagged constructs were efficiently secreted and

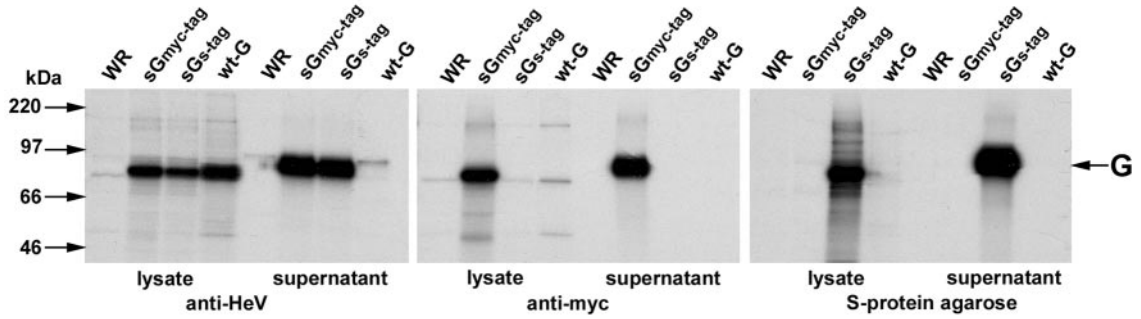

FIG. 2. Expression of recombinant $sG_{S\text{-}tag}$ and $sG_{myc\text{-}tag}$ glycoproteins. HeLa cells were infected with WR, a control vaccinia virus, $sG_{S\text{-}tag}$- or $sG_{myc\text{-}tag}$-encoding viruses, or a recombinant vaccinia virus encoding HeV G and incubated 16 h at 37°C. Beginning at 6 h postinfection, the cells were labeled overnight with [^{35}S]methionine-cysteine. Supernatants were removed and clarified by centrifugation. Lysates were prepared in buffer containing Triton X-100 and clarified by centrifugation. Immunoprecipitations were performed with rabbit anti-HeV or mouse anti-myc MAb 9E10 followed by protein G-Sepharose or with S-protein–agarose. The metabolically labeled proteins were resolved by 10% SDS-PAGE under reducing conditions and detected by autoradiography.

precipitated with whole virus-specific antiserum, we presumed that the addition of the Ig κ leader and the epitope tag did not appear to significantly alter the native structure of G. Moreover, the S-protein agarose affinity precipitations demonstrated high specificity with little nonspecific binding of proteins detected in the control WR or full-length HeV G samples. There was also more $sG_{S\text{-}tag}$ recovered in comparison to $sG_{myc\text{-}tag}$, perhaps due to a higher affinity of the S-protein agarose and S-peptide interaction, and the $sG_{S\text{-}tag}$ could also be detected and purified without a need for specific MAb.

Characterization of soluble HeV G. We next sought to determine if the secreted sG was oligomeric in nature. The apparent molecular weight of purified sG material was first examined using size exclusion chromatography with a calibrated Superdex 200 analytical grade column 10/300. A 500-μg aliquot of affinity-purified $sG_{S\text{-}tag}$ was passed over the Superdex 200, and fractions were collected using the same methods employed for the molecular weight standards. The locations of the protein standards and the elution profile of purified sG are shown in Fig. 3A. Figure 3B shows the analysis of the sG from several fractions across the elution profile separated by 3-to-8% gradient SDS-PAGE under both reducing and nonreducing conditions. These results demonstrate tetrameric, dimeric, and monomeric species of sG. In addition, we note that the majority of sG comprising the bulk of both the first and second peak zones appears as an SDS-stable dimer, which can be seen in fractions 42, 45, and 48. Further, in order to visualize each of the sG species with comparative intensities by staining (Fig. 3B), only 10 μl of 1.0-ml fractions of numbers 42, 45, and 48 were precipitated with S-agarose for both the unreduced and reduced SDS-PAGE analysis, whereas for fraction 39, 0.5 ml was precipitated for both the unreduced and reduced SDS-PAGE analysis, and for fractions 52 and 54 20 μl was used. Thus, only the first portion of peak 1 contains a mixture of a small amount of tetramer with dimer, the majority of the sG glycoprotein is a dimer contained in both peaks 1 and 2, and the final eluted material in the trailing fractions of peak 2 (shown with fractions 52 and 54) is monomeric sG. The apparent overlapping regions of the dimeric sG glycoprotein could be the result of small differences in glycosylation. The estimated molecular masses by size exclusion chromatography of each of the selected fractions are shown in panel A of the figure. The analysis of purified $sG_{S\text{-}tag}$ observed in multiple independent separation experiments indicated an apparent molecular mass range from ~372 ± 19 kDa to ~261 kDa ± 47 kDa (both peaks 1 and 2). The small amount of tetrameric sG elutes with an estimated molecular mass of ~542 ± 20 kDa. A similar elution profile is observed with lectin affinity-purified $sG_{myc\text{-}tag}$ when separated on the Superdex 200 column (not shown). However, from prior experience in the preparation and analysis of engineered soluble virus-derived membrane glycoproteins, such as gp120 from human immunodeficiency virus type 1, the molecular mass calculations derived from size exclusion chromatography analysis are likely overestimated. Specifically, the human immunodeficiency virus type 1 gp120 glycoproteins (~120 kDa in SDS-PAGE) from multiple isolates have apparent molecular masses of >210 kDa when separated on Superdex 200 and are generally in agreement with data from other groups (11, 41). Not surprisingly, the apparent molecular masses of the sG species derived by size exclusion chromatography are about twice those observed by SDS-PAGE. Nevertheless, these results clearly demonstrate that the majority of the soluble and secreted G glycoprotein is oligomeric and appears to be a dimer.

To further characterize the oligomeric species of sG, we separated purified $sG_{S\text{-}tag}$ using sucrose gradient centrifugation. Figure 4 depicts the oligomeric profiles of $sG_{S\text{-}tag}$ on 5-to-20% continuous sucrose gradients. Nonmetabolically labeled sG was harvested from cultures of HeLa cells expressing the protein under serum-free conditions as detailed in Materials and Methods. The supernatant was clarified by centrifugation, buffer exchanged into PBS, and concentrated 40-fold using centrifugal filter units. Approximately 100 μg was divided in two equal portions of 0.5 ml each. One portion was cross-linked with the reducible reagent DTSSP at a final concentration 4 mM, and each of the sG preparations was overlaid and separated on 5-to-20% continuous sucrose gradients. After fractionation of each gradient, the fractions were split into two tubes, precipitated with S-protein–agarose, washed, resuspended, and boiled in SDS sample buffer, one set with and one set without β-mercaptoethanol, and all four sets of fractions were then analyzed by 4-to-12% gradient SDS-PAGE. Figure

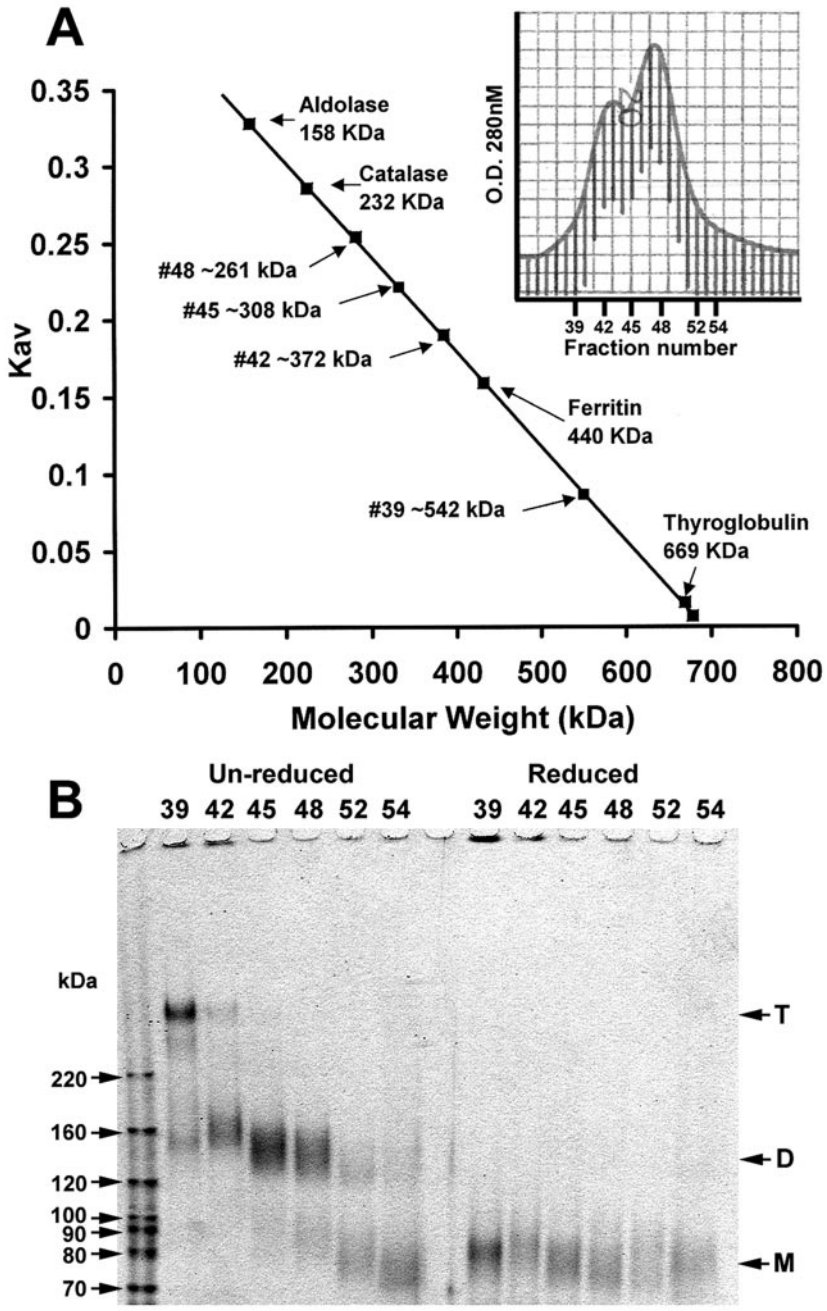

FIG. 3. Size exclusion chromatography analysis of HeV sG. A panel of high-molecular-weight standards was separated on a Superdex 200 size exclusion column, and a calibration curve was generated. Samples of purified $sG_{S\text{-}tag}$ were separated on the calibrated Superdex 200 column and fractionated. A. The Kav values of major sG peaks were calculated, and the apparent molecular weight estimates of several fractions were determined using the calibration curve from the molecular weight standards. The inset in panel A shows the elution profile by absorbance of $sG_{S\text{-}tag}$ and the locations of several individual fractions. B. Selected fractions shown from panel A were analyzed by 3-to-8% gradient SDS-PAGE under both reduced and unreduced conditions and stained with SymplyBlue SaveStain Coomassie G-250. The $sG_{S\text{-}tag}$ species are as follows: M, monomer; D, dimer; T, tetramer.

4A and B are un-cross-linked $sG_{S\text{-}tag}$ separated on the sucrose gradient, fractionated, and affinity precipitated. In Fig. 4A the fractions were prepared in the absence of β-mercaptoethanol, whereas in Fig. 4B the fractions were prepared under reducing conditions with β-mercaptoethanol. Figure 4C and D show cross-linked $sG_{S\text{-}tag}$ separated in a parallel sucrose gradient, fractionated, and affinity precipitated. In Fig. 4C the cross-linked $sG_{S\text{-}tag}$ fractions were prepared in the absence of β-mercaptoethanol, whereas in Fig. 4D each fraction was prepared with β-mercaptoethanol and resolved on the gradient gels. From the data shown in Fig. 4A and C we can determine that for both the un-cross-linked and cross-linked $sG_{S\text{-}tag}$ there are

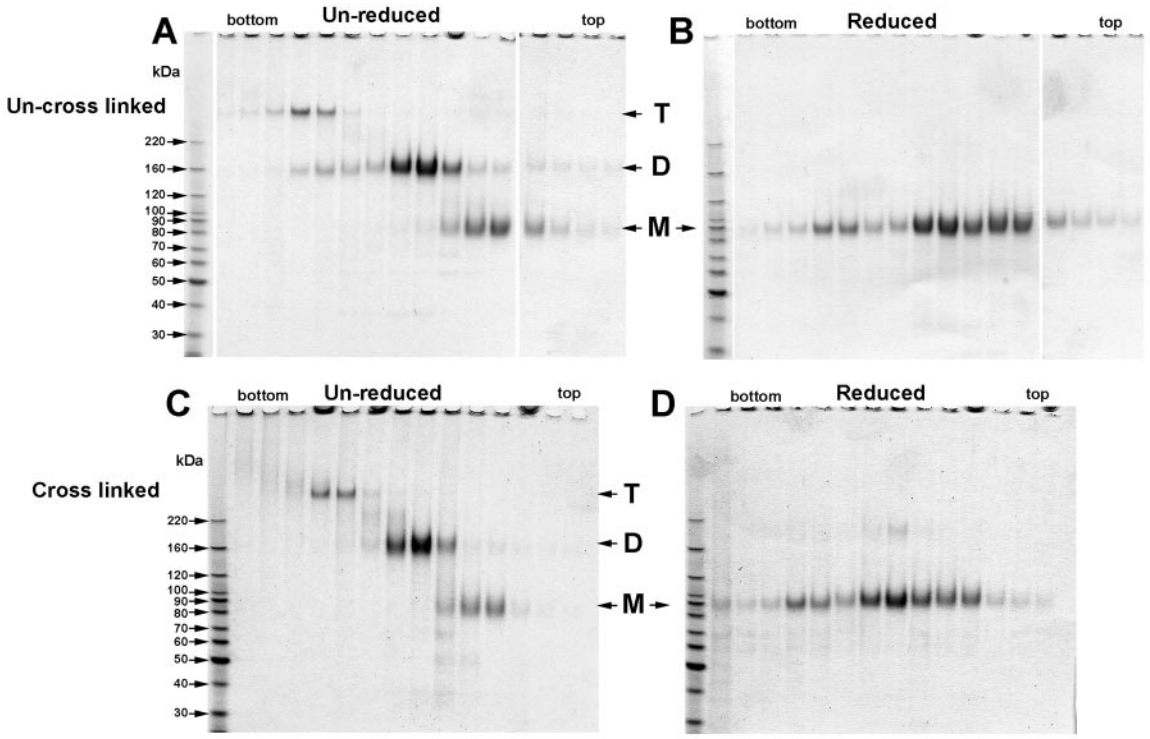

FIG. 4. Oligomeric forms of sG. HeLa cells (two T-162-cm^2 cultures) were infected with $sG_{S\text{-}tag}$-encoding vaccinia virus and incubated for 40 h at 37°C in serum-free OptiMEM medium. Supernatants were removed (40 ml), clarified by centrifugation, concentrated, and buffer exchanged into PBS to a final volume of 1.0 ml. One-half (0.5 ml) of the $sG_{S\text{-}tag}$ was then cross-linked with the reducible reagent DTSSP as described in Materials and Methods and quenched with 100 mM Tris, pH 7.5. The cross-linked and un-cross-linked preparations were layered onto continuous (5-to-20%) sucrose gradients (two gradients) and fractioned. All fractions were precipitated with S-protein agarose, split into two tubes (for reducing and nonreducing SDS-PAGE conditions), and boiled in SDS sample buffer with and without β–mercaptoethanol, the sG products were resolved by 4-to-12% gradient SDS-PAGE, and the protein was visualized by staining with SymplyBlue SaveStain Coomassie G-250. The bottom and top of the gradient fractions are indicated. (A) Non-cross-linked and unreduced; (B) non-cross-linked and reduced; (C) cross-linked and unreduced; (D) cross-linked and reduced. The $sG_{S\text{-}tag}$ species are as follows: M, monomer; D, dimer; T, tetramer.

three distinct species of sG present. Based on the apparent molecular weights of sG in each of the fractions across each of the gradients, these three species represent monomer, dimer, and most likely tetramer. In addition, the immediate cross-linking of the sG with DTSSP prior to sucrose gradient centrifugation did not significantly alter its oligomeric profile and revealed that only a small portion of tetrameric sG is an SDS-sensitive dimer of dimers. The comparative analysis of the non-cross-linked, unreduced, and reduced sG indicates that the sG dimer is disulfide linked, which we anticipated based on data derived from several other paramyxovirus attachment glycoproteins (24, 27). The dimers of other paramyxovirus attachment glycoproteins have also been shown to exist as tetramers and dimers on the surface of infected cells, and it is generally believed that the native oligomeric structure of the paramyxovirus attachment glycoprotein is a dimer of dimers. In addition, the tetrameric species sG we observed also appears to be disulfide linked and is stable when boiled in SDS sample buffer. To contrast these observations on sG to the native full-length G glycoprotein, we expressed and metabolically labeled full-length HeV G in HeLa cells (a receptor-negative cell line) and performed a similar cross-linking experiment and sucrose gradient analysis. Following the cross-linking procedure, or no treatment, of surface-expressed HeV G on intact cells, the cells were lysed with nonionic detergent, lysates were clarified by centrifugation, and each preparation was analyzed by sucrose gradient centrifugation. Fractions were immunoprecipitated with a polyclonal anti-HeV G mouse serum followed by protein G-Sepharose and resolved on 3-to-8% gradient SDS-PAGE under reducing and nonreducing conditions. Shown in Fig. 5 are the results of sucrose gradient analysis of surface-expressed un-cross-linked full-length metabolically labeled HeV G. Here we observed that in the nonreduced fractions, ~70% of the full-length HeV G exists as the apparent tetrameric species (Fig. 5A, lanes 2 to 5), and this oligomeric species is also clearly dependent on disulfide bonds as illustrated by the corresponding reduced fractions which are monomeric (Fig. 5B, lanes 2 to 5). Parallel sucrose gradient analysis of DTSSP (1 mM) cross-linked G resulted in the majority of the dimer migrating at ~160 kDa shifting to the tetramer position in the gradient gel (Fig. 5C). The calculation of the ratios of tetramer to dimer in the un-reduced samples in these first 4 lanes of the gradient gel analysis of the cross-linked G shows a range of 2.2 to 2.8 (Fig. 5C), whereas those ratios in the un-cross-linked G in those lanes (Fig. 5A) range from 1.3 to 1.5. These results strongly suggest that the natural oligomeric form of G in the membrane is a tetramer or dimer of dimers and because of the stability of some of the non-cross-

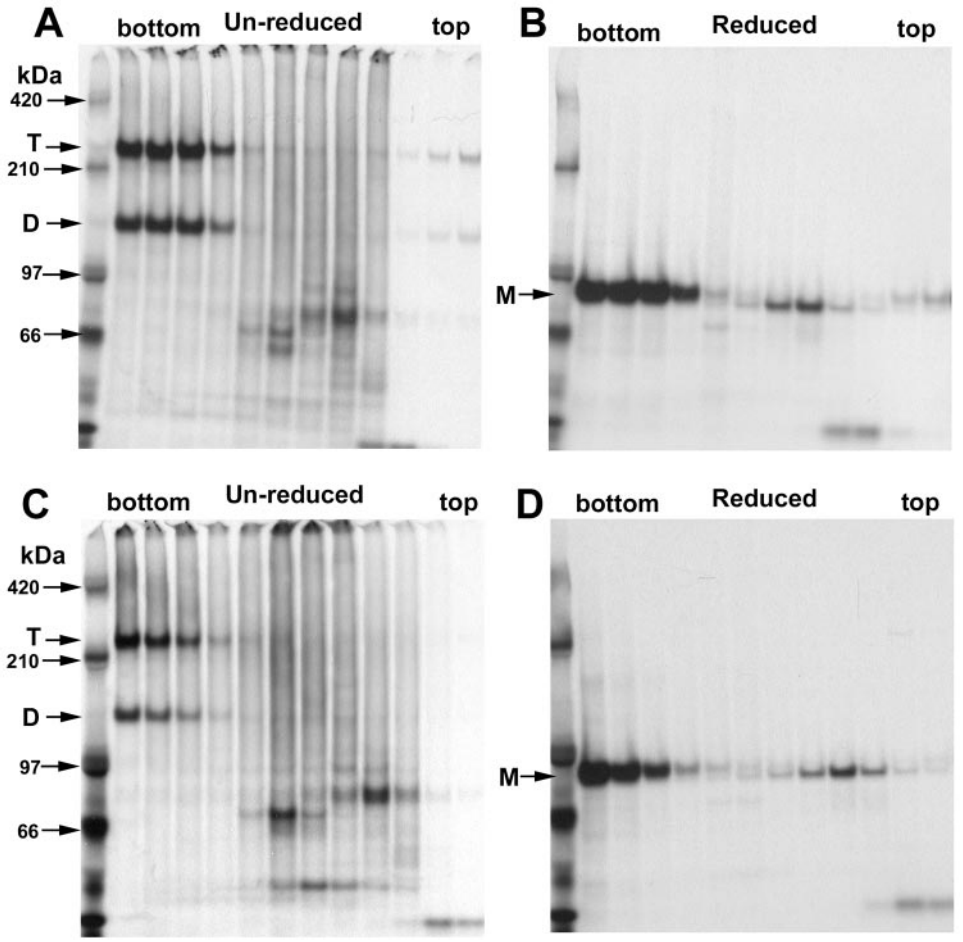

FIG. 5. Oligomeric forms of full-length HeV G. HeLa cells were infected with HeV G-encoding vaccinia virus and incubated for 18 h at 37°C. Beginning at 6 h postinfection, the cells were metabolically labeled overnight with [^{35}S]methionine. Supernatants were removed, and cells were chased for 2 h in complete medium, washed twice in PBS, and recovered. One-half (0.2 ml) of the cell suspension was cross-linked with 1 mM DTSSP as described in Materials and Methods. The cross-linked and non-cross-linked HeV G-expressing cells were lysed in Triton-X buffer and clarified by centrifugation, and each portion was layered onto a continuous sucrose gradient (5 to 20%) and fractioned. The fractions were precipitated with an anti-HeV $sG_{S\text{-}tag}$ mouse antiserum followed by protein G-Sepharose, and all fractions were split into two tubes (for reducing and nonreducing SDS-PAGE conditions). The samples of metabolically labeled HeV G were boiled in SDS sample buffer with and without β-mercaptoethanol, resolved by 3-to-8% gradient SDS-PAGE, and visualized by autoradiography. The bottom and top of the gradient fractions are indicated. (A) Non-cross-linked and unreduced; (B) non-cross-linked and reduced; (C) cross-linked and unreduced; (D) cross-linked and reduced.

linked tetramer complexes when boiled and analyzed by SDS-PAGE under nonreducing conditions, suggests that there may be disulfide bonds linking them together. Repeated experiments using higher amounts of DTSSP (3 and 4 mM) resulted in higher molecular weight aggregates which could not be satisfactorily resolved in the gel unless treated with reducing reagent. In contrast, depending on the particular preparation, the majority (~80 to 90%) of the engineered $sG_{S\text{-}tag}$ glycoprotein released from expressing cells is oligomeric, of which ~95% is dimer and ~5% tetramer, and suggests that it may retain important and useful native structural features.

Immunofluorescence staining of receptor-positive cells by soluble HeV G. Previously, we identified putative receptor-positive and receptor-negative cell types based on their ability to support HeV- and NiV-mediated fusion (6, 7). HeLa cells were the first putative receptor-negative cell line identified, and our data were further confirmed by the resistance to infection by HeV and NiV (unpublished data). Of all the cell lines examined to date, human U373 and PCI 13 have exhibited the highest levels of both HeV- and NiV-mediated fusion and may have a corresponding high level of surface-expressed viral receptor. Vero cells used to grow and maintain HeV and NiV stocks are also fusion permissive. Since G mediates binding to the host cell, we used our $sG_{S\text{-}tag}$ construct in an adapted indirect IFA to show specific binding to receptor-positive cells, the results of which are shown in Fig. 6. Cells were cultivated in Lab-Tek II chamber slides for 3 days and then briefly fixed with acetone. The cells were stained as described in Materials and Methods. The anti-HeV G peptide-specific rabbit serum was used because it does not block HeV-mediated fusion (data not shown) and, therefore, should not interfere with the interaction of $sG_{S\text{-}tag}$ and its putative receptor. In Fig. 6A, the anti-HeV G peptide-specific rabbit antiserum was omitted from each of the cell types stained to show any nonspecific

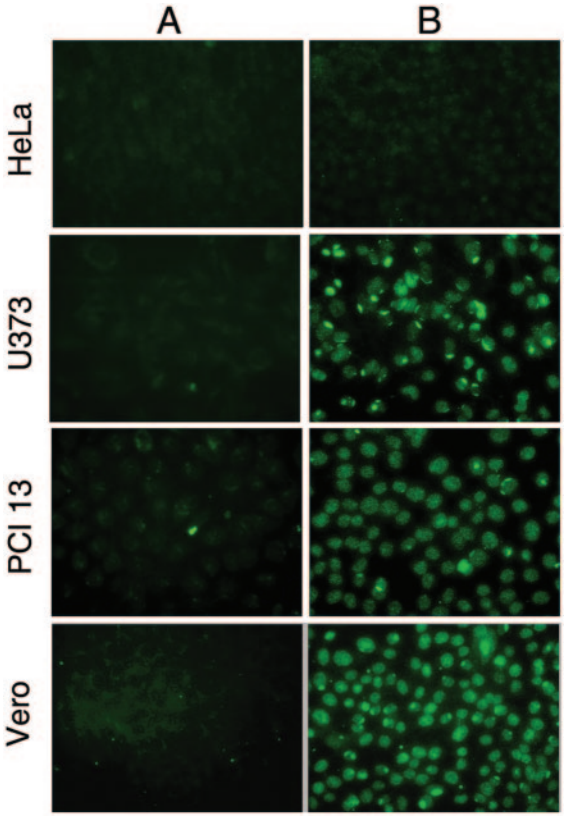

FIG. 6. Immunofluorescence staining of receptor-negative and -positive cells. Cells were plated into eight-well Lab-Tek II chamber slides in the appropriate medium and incubated for 3 days. The cells were fixed with acetone for 2 min. HeLa cells represent a fusion-nonpermissive cell line, whereas U373, PCI 13, and Vero cells represent fusion-permissive cell lines. The cells were stained with $sG_{S\text{-}tag}$ followed by an anti-HeV G peptide-specific rabbit antiserum and a donkey anti-rabbit Alexa Fluor 488 conjugate. Samples were examined with an Olympus microscope with a reflected light fluorescence attachment and an Olympus U-M41001 filter. All images were obtained with a SPOT RT charge-coupled device digital camera at an original magnification of ×40. A. $sG_{S\text{-}tag}$ and donkey anti-rabbit Alexa Fluor 488 conjugate. B. $sG_{S\text{-}tag}$, anti-HeV G peptide-specific antiserum, and donkey anti-rabbit Alexa Fluor 488 conjugate.

staining of the cells by $sG_{S\text{-}tag}$ or the fluorescent conjugate. In Fig. 6B each of the cell types was stained with $sG_{S\text{-}tag}$, the anti-HeV G peptide-specific rabbit antiserum, and the anti-rabbit conjugate. Clearly, $sG_{S\text{-}tag}$ bound to the receptor-positive cells, U373, PCI 13 and Vero, whereas the HeLa cells did not show any positive staining. These data strongly suggest that the $sG_{S\text{-}tag}$ can specifically bind to its host cell receptor and that the HeLa cell line we routinely employ in our studies does not express a functional receptor.

Soluble HeV G blocks virus-mediated cell fusion. HeV- and NiV-mediated fusion have identical cell tropism characteristics, suggesting that these viruses use the same host cell receptor (7). Since $sG_{S\text{-}tag}$ could bind the viral receptor, we hypothesized that sG should therefore be capable of blocking HeV and NiV cell fusion. Using our HeV and NiV cell fusion reporter gene assay, we assessed the inhibitory activity of sG. Figure 7 shows the quantitation of cell fusion reactions mediated by HeV and NiV glycoproteins in the presence of $sG_{S\text{-}tag}$. All supernatants or purified sG were added to target cells for 30 min at 37°C prior to the addition of effector cells. The data shown in Fig. 7A and B were generated using a $sG_{S\text{-}tag}$ supernatant and a WR-infected culture supernatant (control), which were collected and processed identically. The culture supernatants were diluted and added to either U373 (Fig. 7A) or PCI 13 (Fig. 7B) target cells. $sG_{S\text{-}tag}$ was capable of inhibiting HeV-mediated fusion in a dose-dependent manner, whereas the WR supernatant had no effect. In Fig. 7C and D, purified $sG_{S\text{-}tag}$ was tested for its ability to inhibit HeV- and NiV-mediated fusion in both U373 (Fig. 7C) and PCI 13 (Fig. 7D) cells, and it was capable of potently inhibiting HeV-mediated fusion in both cell lines. As expected, NiV-mediated fusion was also inhibited, providing further evidence of a shared cellular receptor. The IC_{50}s of sG in these experiments ranged from 0.2 to 0.4 μg/ml with U373 cells and 0.8 to 3.0 μg/ml with PCI 13 cells for NiV and HeV infection, respectively. Like $sG_{S\text{-}tag}$, lectin-purified $sG_{myc\text{-}tag}$ was also capable of inhibiting both HeV- and NiV-mediated fusion in a dose-dependent manner (data not shown).

Inhibition of HeV and NiV infection by soluble HeV G. We next evaluated the $sG_{S\text{-}tag}$ effects on live virus infection of Vero cells in culture. Here, following preincubation of Vero cells with various concentrations of $sG_{S\text{-}tag}$, the cells were infected with 1.5×10^3 $TCID_{50}$/ml and 7.5×10^2 $TCID_{50}$/ml of live HeV or NiV, respectively, in the presence of $sG_{S\text{-}tag}$ for 30 min, followed by removal of the virus inoculum and incubation with $sG_{S\text{-}tag}$. After 24 h in culture, the number of HeV and NiV infection foci was quantified by specific immunostaining of cell monolayers with a cross-reactive anti-phosphoprotein (P) antiserum as detailed in Materials and Methods. Representative examples of infected Vero cells in the presence or absence of $sG_{S\text{-}tag}$ are shown in Fig. 8. Typically, infection of Vero cells with live HeV or NiV produces characteristic syncytium morphologies for each virus. Immunofluorescence for HeV P protein in HeV syncytia demonstrated that HeV reproducibly infects and incorporates surrounding cells into each syncytium, with cell nuclei and viral protein equally detectable throughout the majority of infected cells (Fig. 8A). NiV-infected cells initially showed a similar appearance to HeV syncytia, but ultimately incorporated nuclei within each giant cell were sequestered together towards the periphery while the remaining cellular debris was also arranged around the outside, leaving the central region largely empty. Thus, immunofluorescence for NiV P protein in NiV syncytia often appears as hollow spheres coated in viral antigen (Fig. 8B) and, by comparison, the untreated control HeV infections produce smaller syncytia relative to the untreated NiV control (Fig. 8A and B). Figure 8C and D are representative examples of HeV- and NiV-infected Vero cells in the presence of 100 μg/ml $sG_{S\text{-}tag}$. Although there were still some infected cells present as detected by immunofluorescence, syncytium formation was completely blocked in both HeV- and NiV-infected cells (Fig. 8C and D, respectively). Furthermore, quantitative analysis of the inhibition of HeV and NiV infection by purified $sG_{S\text{-}tag}$ glycoprotein revealed a dose-dependent response, further demonstrating its specificity, as shown in Fig. 9. Together these data provide strong evidence that HeV and NiV utilize a common receptor on the surface of the host cell. Additionally, the specific inhibition of both viruses by $sG_{S\text{-}tag}$ further demonstrated that the

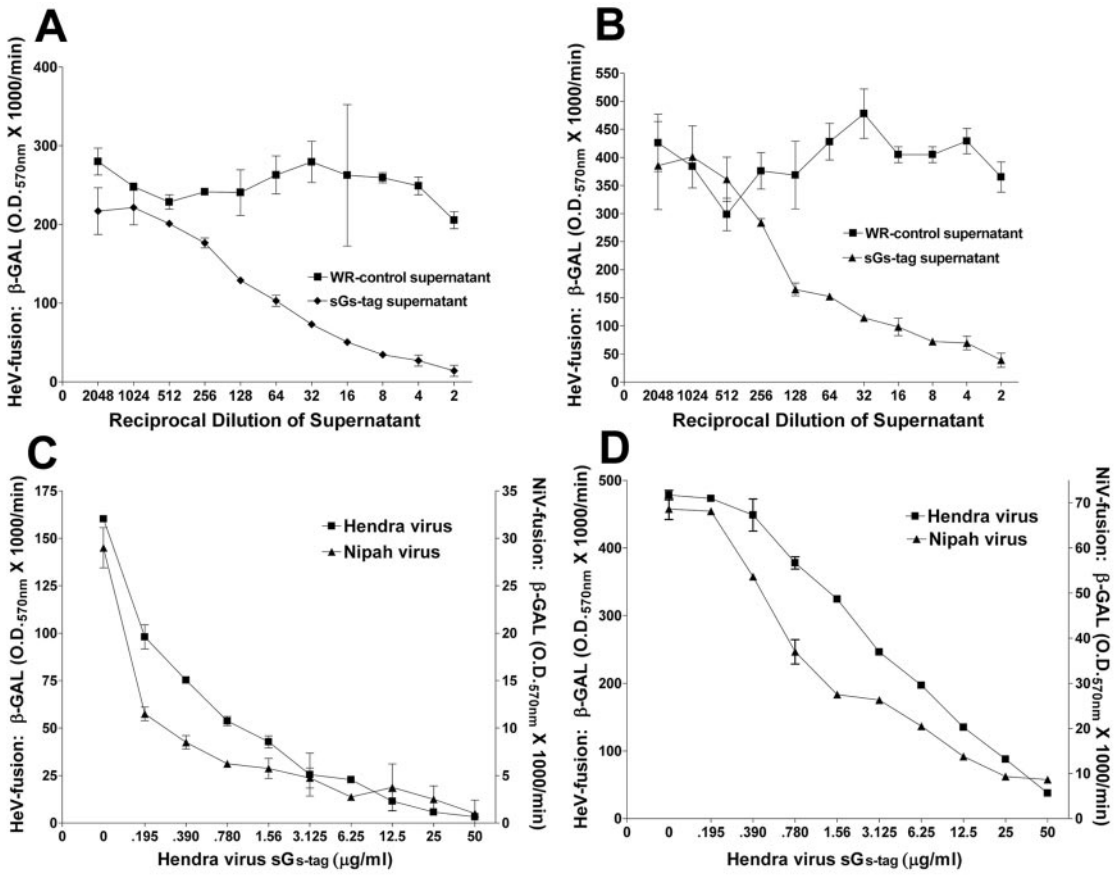

FIG. 7. Inhibition of HeV- and NiV-mediated fusion by sG. HeLa cells were infected with vaccinia virus recombinants encoding HeV F and HeV G or NiV F and NiV G glycoproteins, along with a vaccinia recombinant encoding T7 RNA polymerase (effector cells). Each designated target cell type was infected with the *E. coli* LacZ-encoding reporter vaccinia virus vCB21R. Each target cell type (1×10^5) was plated in duplicate wells of a 96-well plate. Inhibition was carried out using either cell culture supernatants from either $sG_{S\text{-}tag}$-expressing or control vaccinia virus-infected HeLa cell cultures (prepared from 36-h infections), or with purified $sG_{S\text{-}tag}$ preparations at the concentrations indicated, and incubated for 30 min at 37°C. The HeV or NiV glycoprotein-expressing cells (1×10^5) were then mixed with each target cell type. The cell fusion assay was performed for 2.5 h at 37°C, followed by lysis in Nonidet P-40 (1%), and β-Gal activity was quantified. (A and B) Inhibition of HeV-mediated fusion by $sG_{S\text{-}tag}$ supernatant or WR control supernatant in U373 (A) or PCI 13 (B) cells. (C and D) Inhibition of HeV- and NiV-mediated fusion by $sG_{S\text{-}tag}$ in U373 (C) or PCI 13 (D) cells.

$sG_{S\text{-}tag}$ construct maintains important native structural elements. Interestingly, HeV infection was inhibited significantly better than NiV, such that the IC_{50} determined for $sG_{S\text{-}tag}$ was fourfold greater for NiV (13.20 μg/ml) than for HeV (3.3 μg/ml) (Fig. 9). Given the current evidence suggesting both viruses utilize a common receptor, the reasons for the differences observed in $sG_{S\text{-}tag}$ inhibition of virus infection versus cell fusion remain unknown. We did not observe a similar difference in the ability of $sG_{S\text{-}tag}$ to inhibit HeV- and NiV-mediated cell fusion, as demonstrated in Fig. 6. Although HeV-mediated fusion was more potent than NiV-mediated fusion, illustrated by the higher levels of substrate turnover, the $sG_{S\text{-}tag}$ IC_{50} in both cell fusion assays remained constant. In previous reports we have demonstrated through heterotypic function that the difference in cell fusion rates between HeV and NiV was dependent on the fusion protein. In this study, we demonstrated that natural NiV infection appears to be more vigorous than HeV infection. We can only speculate that other viral proteins present during infection are perhaps influencing the kinetics of infection, thus altering the inhibition susceptibility, or there may be differences in the affinities of HeV sG versus NiV G to the cell surface-expressed receptor.

Soluble HeV G elicits a potent virus-neutralizing polyclonal antibody response. With few exceptions, it is the envelope glycoproteins of viruses to which virtually all neutralizing antibodies are directed and all successful human viral vaccines induce neutralizing antibodies that can cross-react with immunologically relevant strains of a virus (34). More specifically, virus-neutralizing antibodies are the key vaccine-induced protective mechanism in the case of the paramyxoviruses mumps and measles (reviewed in references 20 and 30), and it has been shown that vaccinia virus-expressed full-length envelope glycoproteins from NiV can elicit virus-neutralizing antibodies (38). Our data indicate that the $sG_{S\text{-}tag}$ glycoprotein retains important structural features based on its abilities to specifically bind receptor-positive cells and block both HeV- and NiV-mediated fusion and infection. Thus, the immunization of animals with sG should potentially generate potent virus-neutralizing antibodies. To test this possibility, purified $sG_{S\text{-}tag}$ was used to immunize rabbits, and the resulting anti-G antiserum

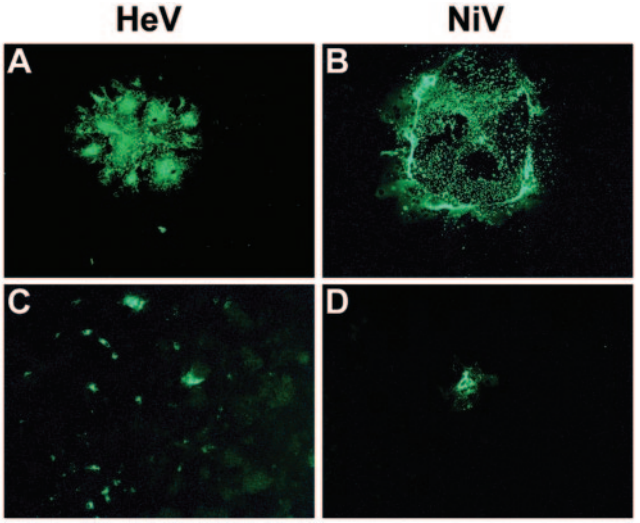

FIG. 8. Immunofluorescence-based syncytium assay of HeV and NiV. Vero cells were plated into 96-well plates and grown to 90% confluence. Cells were pretreated with $sG_{S\text{-}tag}$ for 30 min at 37°C prior to infection with 1.5×10^3 $TCID_{50}$/ml and 7.5×10^2 $TCID_{50}$/ml of live HeV or NiV (combined with $sG_{S\text{-}tag}$). Cells were incubated for 24 h, fixed in methanol, and immunofluorescently labeled for P protein prior to digital microscopy. Images were obtained using an Olympus IX71 inverted microscope coupled to an Olympus DP70 high-resolution color camera, and all images were obtained at an original magnification of ×85. Shown are representative images of FITC immunofluorescence of anti-P-labeled HeV and NiV. (A) Untreated HeV control infections; (B) untreated NiV control infections; (C) HeV infections in the presence of 100 μg/ml $sG_{S\text{-}tag}$; (D) NiV infections in the presence of 100 μg/ml $sG_{S\text{-}tag}$.

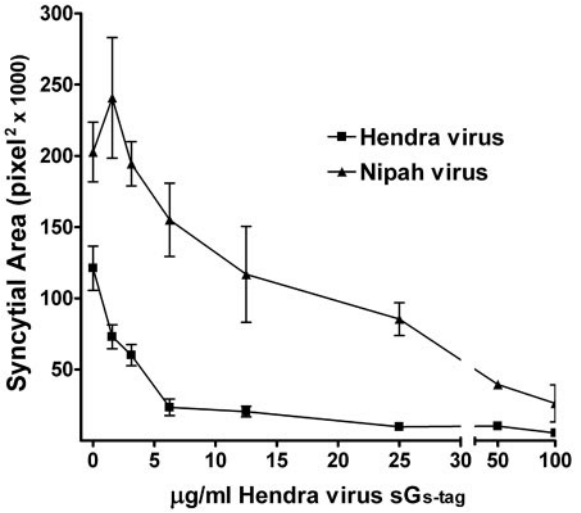

FIG. 9. Inhibition of HeV and NiV infection by sG. Vero cells were plated into 96-well plates and grown to 90% confluence. Cells were pretreated with $sG_{S\text{-}tag}$ for 30 min at 37°C prior to infection with 1.5×10^3 $TCID_{50}$/ml and 7.5×10^2 $TCID_{50}$/ml of live HeV or NiV (combined with $sG_{S\text{-}tag}$). Cells were incubated for 24 h, fixed in methanol, and immunofluorescently labeled for P protein prior to digital microscopy and image analysis to determine the relative area of each syncytium (see Materials and Methods). The figure shows the relative syncytial area (pixels squared) versus $sG_{S\text{-}tag}$ concentration for HeV (circles) and NiV (triangles).

was evaluated in virus neutralization assays with both HeV and NiV. Table 1 summarizes the neutralization of HeV and NiV infection by the polyclonal rabbit anti-G sera. The sera from both rabbits were capable of complete neutralization of HeV at a dilution of 1:1,280. NiV was also neutralized by the $sG_{S\text{-}tag}$ antiserum, with complete neutralization at a dilution of 1:640. A twofold difference in titer is consistent with partial antibody cross-reactivity of the HeV and NiV G glycoproteins. Prebleeds from both rabbits were also tested for their abilities to neutralize HeV and NiV. Although there was slight neutralization at the highest concentration, this activity was completely abrogated upon dilution of the sera (data not shown). Previous studies have demonstrated that HeV and NiV antisera do cross-neutralize, with each serum being slightly less effective against the heterotypic virus (13, 38). Moreover, in previous work we demonstrated a similar trend in cross-neutralization in a cell fusion assay for HeV and NiV (6, 7). Because $sG_{S\text{-}tag}$ is able to elicit such a potent immune response with high levels of neutralizing antibodies, it may provide an avenue for vaccine development strategies.

DISCUSSION

Previously, we examined the functional activities of the fusion and attachment envelope glycoproteins of HeV and NiV by using a vaccinia virus-based expression system and a quantitative assay for measuring membrane fusion. These studies revealed the same pattern of host-cell tropism for both HeV- and NiV-mediated fusion, suggesting that these closely related viruses utilize the same host cell receptor for infection (6, 7). The receptor for HeV and NiV is likely a specific cell surface-expressed protein, and there are several lines of evidence to support this notion. First, HeV does not contain any hemagglutinating activity (28) or neuraminidase activity (42). In addition, neuraminidase treatment of Vero cells (the cell line used to propagate HeV and NiV stocks) does not inhibit HeV or NiV infection or cell fusion, but it can abrogate their susceptibility to Newcastle disease virus and influenza virus A, two

TABLE 1. Neutralization of HeV and NiV infection[a]

Dilution	HeV		NiV	
	Rabbit 405	Rabbit 406	Rabbit 405	Rabbit 406
1:10	− −	− −	− −	− −
1:20	− −	− −	− −	− −
1:40	− −	− −	− −	− −
1:80	− −	− −	− −	− −
1:160	− −	− −	− −	− −
1:320	− −	− −	− −	− −
1:640	− −	− −	− −	− −
1:1,280	− −	− −	+ +	− +
1:2,560	− −	− +	+ +	+ +
1:5,120	− −	+ +	+ +	+ +
1:10,240	+ +	+ +	+ +	+ +
1:20,480	+ +	+ +	+ +	+ +

[a] Anti-HeV G antisera were generated in rabbits by three inoculations with purified $sG_{S\text{-}tag}$. Sera collected 2 weeks after the third injection were analyzed in a virus neutralization assay against HeV and NiV. Serum neutralization titers (in duplicate) were determined by the presence of CPE (indicated by +) and recorded as the serum dilution where at least one of the duplicate wells showed CPE. −, no CPE.

viruses which employ sialic acid as receptors (16). Also, certain cell lines from the same species, most notably human cell lines, can be clearly positive or negative for fusion, and protease treatment prevents fusion of an otherwise permissive target cell (6, 7, 16). To further characterize the HeV attachment G glycoprotein and its unknown host cell receptor, we have constructed two soluble forms of the protein (sG).

The first description of an engineered soluble and secreted type II membrane glycoprotein from a virus was derived by a novel strategy whereby the signal sequence and membrane anchor domain elements of the influenza virus neuraminidase glycoprotein were replaced with the hydrophobic amino-terminal domain of the F_1 subunit of the SV5 F glycoprotein, which could serve as a signal peptide (32). Using a similar strategy, the HN glycoprotein of SV5, another type II membrane glycoprotein, was successfully engineered into a soluble and secreted product (31). Aside from HeV and NiV, the only other paramyxovirus possessing a G envelope glycoprotein as its attachment glycoprotein is respiratory syncytial virus (RSV) (reviewed in reference 21). However, the HeV and NiV G glycoproteins are quite distinct from RSV G, lacking homology and, at 604 and 602 amino acids, respectively, double the length of RSV G (reviewed in references 22 and 40). It has been previously observed that RSV can produce both a membrane-associated and a secreted truncated form of its attachment G glycoprotein, where alternative methionine start sites are utilized (25, 35). Our initial attempts to design a soluble HeV G construct implemented either a truncation strategy of the molecule's N terminus or a sequential deletion strategy through the TM based on the observations of soluble RSV G, but these attempts proved unsuccessful. Here we devised a mutagenesis strategy whereby the protein's predicted signal sequence, cytoplasmic tail, and transmembrane domains were replaced with an Ig κ leader signal sequence coupled to either an S-peptide tag ($sG_{S\text{-}tag}$) or the myc epitope tag (sG_{myc}) to facilitate purification and detection.

These constructs were efficiently expressed, and the sG glycoprotein products could be readily purified from the culture supernatants of cells infected with an sG-encoding vaccinia virus. Although both tagged versions appeared to be expressed equally well, were oligomeric, were recognized by polyclonal anti-HeV antiserum, and could block HeV and NiV cell fusion, we found that the $sG_{S\text{-}tag}$ version was more readily expressed and purified to higher levels in a cost-effective manner using S-protein affinity matrices than the myc-tagged version of sG. Analysis of purified sG by fractionation using sucrose gradient centrifugation and analysis by gradient SDS-PAGE under both reducing and nonreducing conditions revealed a monomeric species of ~80 kDa, a dimeric species of ~160 kDa, and a tetrameric species migrating well above the 220-kDa marker. In parallel, experiments conducted in conjunction with the use of a reducible cross-linking reagent on sG revealed that only a small portion of the tetrameric sG is an SDS-sensitive dimer of dimers, whereas the majority of tetrameric sG is stable even when boiled in SDS under nonreducing conditions without the addition of chemical cross-linking. The cross-linking studies also revealed that the majority of the monomeric and dimeric sG glycoproteins are present as separate species and do not cross-link to higher molecular forms. Thus, a significant portion of the sG glycoprotein is released from cells and can be purified as an oligomeric product. Sucrose gradient fractionation and analysis of full-length HeV G glycoprotein isolated from cells revealed that the majority of the protein is a highly stable tetrameric species with an apparent molecular mass in SDS-PAGE of ~380 kDa. Based on the stability of both the full-length and soluble HeV G dimer and tetrameric species in boiled SDS sample buffer that is observed using SDS-PAGE analysis under nonreducing conditions and in the absence of cross-linker, we conclude that the dimer and some tetramer species are disulfide linked.

The retention of the protein's oligomeric characteristics suggested that the purified sG glycoprotein also retained important biological characteristics as well. Indeed, the sG glycoprotein could specifically bind to the surfaces of cell fusion-permissive cell types, while there was little evidence of binding to fusion-nonpermissive cell types, most notably the HeLa cell line clone used here. Presumably, these binding data are a direct reflection of surface-expressed HeV receptor. These observations were further supported by the ability of the sG glycoprotein preparations to potently block both HeV- and NiV-mediated cell fusion. The mechanism of this inhibition is likely due to occupancy of virus receptor sites on the target cells and further supports the likelihood that both HeV and NiV utilize the same receptor. We confirmed these observations through an examination of the glycoprotein's ability to block infectious virus entry, and we found that it was capable of blocking both HeV and NiV infection of Vero cells. Whether there could be differences in the ability of a dimeric sG versus its monomeric form in the ability to presumably bind cell-surface receptor and block virus-mediated fusion is presently unknown, but it could be that a dimeric form would have greater potency though avidity.

Finally, the sG glycoprotein could serve as a potential subunit vaccine, and we also demonstrated here that administration of HeV sG to rabbits is capable of eliciting a potent and cross-reactive virus-neutralizing antibody response against both HeV and NiV. Taken together, the sG glycoprotein derived from HeV appears to retain several important functional and biochemical characteristics and will facilitate structural studies on this important *Henipavirus* membrane glycoprotein. The optimization of such a soluble glycoprotein strategy to henipavirus vaccine development could prove highly successful as one means of combating these emerging viral threats.

ACKNOWLEDGMENTS

We thank Andrew Hickey for supplying the mouse polyclonal antiserum to soluble HeV G.

This study was supported by NIH AI057168 and USUHS R073IL grants to C.C.B.

The views expressed in the manuscript are solely those of the authors, and they do not represent official views or opinions of the Department of Defense or The Uniformed Services University of the Health Sciences.

REFERENCES

1. **Anonymous.** 2004. Nipah virus outbreak(s) in Bangladesh, January-April 2004. Wkly. Epidemiol. Rec. **79:**168–171.
2. **Anonymous.** 2004. Hendra virus—Australia (Queensland). International Society for Infectious Diseases, 14 Dec. 2004. Pro-med. no. 20041214.3307.
3. **Anonymous.** 2004. Person-to-person transmission of Nipah virus during outbreak in Faridpur District, 2004. ICDDR,B Health Sci. Bull. **2:**5–9.
4. **Berger, E. A., O. Nussbaum, and C. C. Broder.** 1995. HIV envelope glycoprotein/CD4 interactions: studies using recombinant vaccinia virus vectors,

p. 123–145. *In* J. Karn (ed.), HIV: a practical approach, vol. 2. Oxford University Press, Cambridge, United Kingdom.
5. **Bossart, K. N., and C. C. Broder.** 2004. Viral glycoprotein-mediated cell fusion assays using vaccinia virus vectors. Methods Mol. Biol. **269:**309–332.
6. **Bossart, K. N., L.-F. Wang, B. T. Eaton, and C. C. Broder.** 2001. Functional expression and membrane fusion tropism of the envelope glycoproteins of Hendra virus. Virology **290:**121–135.
7. **Bossart, K. N., L. F. Wang, M. N. Flora, K. B. Chua, S. K. Lam, B. T. Eaton, and C. C. Broder.** 2002. Membrane fusion tropism and heterotypic functional activities of the Nipah virus and Hendra virus envelope glycoproteins. J. Virol. **76:**11186–11198.
8. **Broder, C. C., and E. A. Berger.** 1995. Fusogenic selectivity of the envelope glycoprotein is a major determinant of human immunodeficiency virus type 1 tropism for $CD4^+$ T- cell lines vs. primary macrophages. Proc. Natl. Acad. Sci. USA **92:**9004–9008.
9. **Butler, D.** 2004. Fatal fruit bat virus sparks epidemics in southern Asia. Nature **429:**7.
10. **Carroll, M. W., and B. Moss.** 1995. E. coli beta-glucuronidase (GUS) as a marker for recombinant vaccinia viruses. BioTechniques **19:**352–356.
11. **Center, R. J., P. L. Earl, J. Lebowitz, P. Schuck, and B. Moss.** 2000. The human immunodeficiency virus type 1 gp120 V2 domain mediates gp41-independent intersubunit contacts. J. Virol. **74:**4448–4455.
12. **Chua, K. B.** 2003. Nipah virus outbreak in Malaysia. J. Clin. Virol. **26:**265–275.
13. **Crameri, G., L. F. Wang, C. Morrissy, J. White, and B. T. Eaton.** 2002. A rapid immune plaque assay for the detection of Hendra and Nipah viruses and anti-virus antibodies. J. Virol. Methods **99:**41–51.
14. **Crennell, S., T. Takimoto, A. Portner, and G. Taylor.** 2000. Crystal structure of the multifunctional paramyxovirus hemagglutinin-neuraminidase. Nat. Struct. Biol. **7:**1068–1074.
15. **Eaton, B. T.** 2001. Introduction to current focus on Hendra and Nipah viruses. Microbes Infect. **3:**277–278.
16. **Eaton, B. T., P. J. Wright, L. F. Wang, O. Sergeyev, W. P. Michalski, K. N. Bossart, and C. C. Broder.** 2004. Henipaviruses: recent observations on regulation of transcription and the nature of the cell receptor. Arch. Virol. Suppl. **2004 (18):**122–131.
17. **Enserink, M.** 2004. Emerging infectious diseases. Nipah virus (or a cousin) strikes again. Science **303:**1121.
18. **Feng, Y., C. C. Broder, P. E. Kennedy, and E. A. Berger.** 1996. HIV-1 entry cofactor: functional cDNA cloning of a seven-transmembrane, G protein-coupled receptor. Science **272:**872–877.
19. **Fuerst, T. R., E. G. Niles, F. W. Studier, and B. Moss.** 1986. Eukaryotic transient-expression system based on recombinant vaccinia virus that synthesizes bacteriophage T7 RNA polymerase. Proc. Natl. Acad. Sci. USA **83:**8122–8126.
20. **Griffin, D. E.** 1995. Immune responses during measles virus infection. Curr. Top. Microbiol. Immunol. **191:**117–134.
21. **Hacking, D., and J. Hull.** 2002. Respiratory syncytial virus—viral biology and the host response. J. Infect. **45:**18–24.
22. **Harcourt, B. H., A. Tamin, T. G. Ksiazek, P. E. Rollin, L. J. Anderson, W. J. Bellini, and P. A. Rota.** 2000. Molecular characterization of Nipah virus, a newly emergent paramyxovirus. Virology **271:**334–349.
23. **Harrington, R. D., and A. P. Geballe.** 1993. Cofactor requirement for human immunodeficiency virus type 1 entry into a CD4-expressing human cell line. J. Virol. **67:**5939–5947.
24. **Lamb, R. A., and D. Kolakofsky.** 2001. *Paramyxoviridae*: the viruses and their replication, p. 1305–1340. *In* D. M. Knipe and P. M. Howley (ed.), Fields virology, 4th ed. Lippincott Williams & Wilkins, Philadelphia, Pa.
25. **Lichtenstein, D. L., S. R. Roberts, G. W. Wertz, and L. A. Ball.** 1996. Definition and functional analysis of the signal/anchor domain of the human respiratory syncytial virus glycoprotein G. J. Gen. Virol. **77:**109–118.
26. **Morrison, T. G.** 1988. Structure, function, and intracellular processing of paramyxovirus membrane proteins. Virus Res. **10:**113–135.
27. **Morrison, T. G.** 2001. The three faces of paramyxovirus attachment proteins. Trends Microbiol. **9:**103–105.
28. **Murray, K., P. Selleck, P. Hooper, A. Hyatt, A. Gould, L. Gleeson, H. Westbury, L. Hiley, L. Selvey, B. Rodwell, et al.** 1995. A morbillivirus that caused fatal disease in horses and humans. Science **268:**94–97.
29. **Nussbaum, O., C. C. Broder, and E. A. Berger.** 1994. Fusogenic mechanisms of enveloped-virus glycoproteins analyzed by a novel recombinant vaccinia virus-based assay quantitating cell fusion-dependent reporter gene activation. J. Virol. **68:**5411–5422.
30. **Pantaleo, G., and R. A. Koup.** 2004. Correlates of immune protection in HIV-1 infection: what we know, what we don't know, what we should know. Nat. Med. **10:**806–810.
31. **Parks, G. D., and R. A. Lamb.** 1990. Folding and oligomerization properties of a soluble and secreted form of the paramyxovirus hemagglutinin-neuraminidase glycoprotein. Virology **178:**498–508.
32. **Paterson, R. G., and R. A. Lamb.** 1990. Conversion of a class II integral membrane protein into a soluble and efficiently secreted protein: multiple intracellular and extracellular oligomeric and conformational forms. J. Cell Biol. **110:**999–1011.
33. **Plemper, R. K., A. L. Hammond, and R. Cattaneo.** 2000. Characterization of a region of the measles virus hemagglutinin sufficient for its dimerization. J. Virol. **74:**6485–6493.
34. **Quinnan, G. V.** 1997. Immunization against viral diseases, p. 791–834. *In* G. Galasso, R. Whitley, and T. C. Merigan (ed.), Antiviral agents and human viral disease. Raven Press, New York, N.Y.
35. **Roberts, S. R., D. Lichtenstein, L. A. Ball, and G. W. Wertz.** 1994. The membrane-associated and secreted forms of the respiratory syncytial virus attachment glycoprotein G are synthesized from alternative initiation codons. J. Virol. **68:**4538–4546.
36. **Russell, R., R. G. Paterson, and R. A. Lamb.** 1994. Studies with cross-linking reagents on the oligomeric form of the paramyxovirus fusion protein. Virology **199:**160–168.
37. **Sheehan, J. P., R. M. Iorio, R. J. Syddall, R. L. Glickman, and M. A. Bratt.** 1987. Reducing agent-sensitive dimerization of the hemagglutinin-neuraminidase glycoprotein of Newcastle disease virus correlates with the presence of cysteine at residue 123. Virology **161:**603–606.
38. **Tamin, A., B. H. Harcourt, T. G. Ksiazek, P. E. Rollin, W. J. Bellini, and P. A. Rota.** 2002. Functional properties of the fusion and attachment glycoproteins of Nipah virus. Virology **296:**190–200.
39. **Tan, C. T., and K. T. Wong.** 2003. Nipah encephalitis outbreak in Malaysia. Ann. Acad. Med. Singapore **32:**112–117.
40. **Wang, L., B. H. Harcourt, M. Yu, A. Tamin, P. A. Rota, W. J. Bellini, and B. T. Eaton.** 2001. Molecular biology of Hendra and Nipah viruses. Microbes Infect. **3:**279–287.
41. **Yang, X., M. Farzan, R. Wyatt, and J. Sodroski.** 2000. Characterization of stable, soluble trimers containing complete ectodomains of human immunodeficiency virus type 1 envelope glycoproteins. J. Virol. **74:**5716–5725.
42. **Yu, M., E. Hansson, J. P. Langedijk, B. T. Eaton, and L. F. Wang.** 1998. The attachment protein of Hendra virus has high structural similarity but limited primary sequence homology compared with viruses in the genus Paramyxovirus. Virology **251:**227–233.